

BARYON LOADED RELATIVISTIC BLASTWAVES IN SUPERNOVAE

SAYAN CHAKRABORTI¹ & ALAK RAY¹

Department of Astronomy and Astrophysics, Tata Institute of Fundamental Research,
1 Homi Bhabha Road, Mumbai 400 005, India

DRAFT October 12, 2018

ABSTRACT

We provide a new analytic blastwave solution which generalizes the Blandford-McKee solution to arbitrary ejecta masses and Lorentz factors. Until recently relativistic supernovae have been discovered only through their association with long duration Gamma Ray Bursts (GRB). The blastwaves of such explosions are well described by the Blandford-McKee (in the ultra relativistic regime) and Sedov-Taylor (in the non-relativistic regime) solutions during their afterglows, as the ejecta mass is negligible in comparison to the swept up mass. The recent discovery of the relativistic supernova SN 2009bb, without a detected GRB, opens up the possibility of highly baryon loaded mildly relativistic outflows which remains in nearly free expansion phase during the radio afterglow. In this work, we consider a massive, relativistic shell, launched by a Central Engine Driven EXplosion (CEDEX), decelerating adiabatically due to its collision with the pre-explosion circumstellar wind profile of the progenitor. We compute the synchrotron emission from relativistic electrons in the shock amplified magnetic field. This models the radio emission from the circumstellar interaction of a CEDEX. We show that this model explains the observed radio evolution of the prototypical SN 2009bb and demonstrate that SN 2009bb had a highly baryon loaded, mildly relativistic outflow. We discuss the effect of baryon loading on the dynamics and observational manifestations of a CEDEX. In particular, our predicted angular size of SN 2009bb is consistent with VLBI upper limits on day 85, but is presently resolvable on VLBI angular scales, since the relativistic ejecta is still in the nearly free expansion phase.

Subject headings: gamma rays: bursts — supernovae: individual (SN 2009bb) — shock waves — radiation mechanisms: non-thermal — techniques: interferometric

1. INTRODUCTION

Ultra relativistic bulk motion of matter particles in astrophysical settings is implied most notably in Gamma Ray Bursts (GRBs) (see Piran (1999, 2004) for reviews). Afterglows from GRBs are generated from the emission by relativistic shocks that result from slowing down of a relativistic shell by the the medium surrounding the progenitor star that exploded. Similar interaction of stellar material (ejecta) from an exploding star with the circumstellar matter (CSM) gives rise to non-relativistic shocks in core collapse supernovae.

Fluid dynamical treatment of ultra-relativistic spherical blast waves mediated by strong shocks² has been given by Blandford & McKee (1976, 1977). They describe a similarity solution of an explosion of a fixed amount of energy in a uniform medium. This includes an adiabatic blast wave and an impulsive injection of energy on a short timescale as well as an explosion where the total energy increases with time, suggesting that the blast wave has a continuous central power supply. Another important model considered by them is that of a blast wave propagating into a spherically symmetric wind. On the other hand, the initial nearly free ex-

pansion of a non-relativistic supernova blast wave, interacting with the surrounding circumstellar medium, was found by Chevalier (1982); Nadezhin (1985). Once the blast wave sweeps up more CSM material than its own rest mass, the self-similar solutions of non-relativistic blast waves are described in the Newtonian regime by the Sedov (1946) von Neumann (1963) Taylor (1950) solution.

In this paper we provide an analytic solution of the standard model of relativistic hydrodynamics (see e.g. Piran 1999; Chiang & Dermer 1999) for an adiabatic blastwave. Here, the exploding shell decelerates due to inelastic collision with an external medium. That is, we provide the solution for an arbitrary Lorentz factor of the expanding supernova shell. The need for such a solution which can handle a trans-relativistic outflow is motivated by the discovery of SN 2009bb, a type Ibc supernova without a detected GRB which shows clear evidence of a mildly relativistic outflow powered by a central engine (Soderberg et al. 2010). SN 2009bb-like objects (Central Engine Driven Explosions, hereafter CEDEX) differ in another significant way from classical GRBs: they are highly baryon loaded explosions with non-negligible ejecta masses. Our new analytic blastwave solution therefore generalizes the Blandford & McKee (1976) result, in particular their impulsive, adiabatic blast wave in a wind-like $\rho \propto r^{-2}$ CSM.

The new class of relativistic supernovae without a detected GRB, e.g. SN 2009bb, relaxes two important and well-known constraints of the GRBs, namely the *compactness problem* and *baryon contamination*. Thus highly baryon loaded mildly relativistic outflows can re-

sayan@tifr.res.in, akr@tifr.res.in

¹ Also at Institute for Theory and Computation, Harvard-Smithsonian Center for Astrophysics, 60 Garden St., Cambridge, MA 02138, USA

² Here the strong shocks are those where the random kinetic energy per particle behind the shock is much greater than the unshocked medium, i.e., $p_2/n_2 \gg p_1/n_1$, the subscripts 2 and 1 denote the shocked gas and unshocked gas respectively and p, n are the pressure and number densities.

main in the nearly free expansion phase during the radio afterglow. Therefore we consider the evolution of a massive relativistic shell launched by a CEDEX, experiencing collisional slowdown due to interaction with the pre-explosion circumstellar wind of the progenitor. We calculate the time evolution of the radius, bulk Lorentz factor and thermal energy of the decelerating blastwave. Our solution reduces to the Blandford & McKee (1976) solution, in the ultra-relativistic, negligible ejecta mass limit. We also quantify the density of accelerated electrons, amplified magnetic fields and hence the radio synchrotron emission from the blastwave of a CEDEX.

In Section 2 we outline the conditions that require ultra-high bulk Lorentz factors and very low ejecta masses in classical Long GRBs. We argue why these constraints are relaxed in the case of mildly relativistic outflows detected in SN 2009bb like events, that have no detected GRBs. It provides the motivation for the analytic solution derived here. In Section 3 we develop the analytic solution of a relativistic blast wave launched by a CEDEX, for the collisional slowdown model described by Piran (1999). We use this solution to show that the SN 2009bb blast wave is substantially baryon loaded and remains in the nearly free expansion phase throughout the ~ 1 year of observations (Figure 1). In section 4 we discuss the relativistic blast wave energetics. We quantify the amount of shock accelerated electrons and magnetic field amplification in a CEDEX blast wave. In Section 5 we use this information to model the radio spectrum and light curve of a CEDEX in the nearly free expansion phase. In section 6 we provide expressions to deduce the blast wave parameters from the observed radio spectrum. We also compare our blastwave solution to other known solutions relevant for relativistic blastwaves in the literature (Section 7). In section 8 we discuss the implications of baryon loading in determining the evolution and observational signatures of a CEDEX. In the Appendix we provide the analytic expressions for the temporal evolution of the blast wave parameters (Section A). We demonstrate that our solution reduces to the ultra-relativistic Blandford & McKee (1976) solution for a constant velocity wind, in the low mass, ultra-relativistic limit (Section B). In Section C we provide “stir-fry expressions”³ for the radio spectrum of a CEDEX with known initial blast wave parameters. In Section D we invert the problem and provide handy expressions for estimating the initial parameters for a CEDEX from radio observations. In Section E we provide an expression to compute angular size of a CEDEX from multi-band radio spectrum. Using the radio spectrum of SN 2009bb, we show that our predicted angular size is consistent with the reported upper limits (Bietenholz et al. 2010) from VLBI, but should be resolvable presently.

2. RELATIVISTIC OUTFLOW IN GRBS AND CEDEX

Relativistic supernovae have, until recently, been discovered only through their temporal and spatial associ-

³ We note that a similar term “TV Dinner Equations” appeared in the Astrophysical literature in a paper on GRBs (Rhoads 1999) to denote equations where “numerical values for physical constants have been inserted, so they are ready to use without further preparation”; in the present work, “stir-fry” expressions would allow users to pick and choose usable formulae derived or approximated in this work and quickly (re)assemble their own combination of useful input parameters.

ation with long duration GRBs. An acceptable model for GRBs must find a way to circumvent the *compactness* and *baryon contamination* problems. The observed rapid temporal variability in GRBs imply a very compact source. The compactness problem pointed out by Ruderman (1975) and Schmidt (1978), indicates that γ -ray photons of sufficiently high energies will produce electron-positron pairs and will not be able to come out due to the resulting high opacity. However, the observation of high energy photons from GRBs was reconciled with such theoretical constraints by Goodman (1986) and Paczynski (1986), allowing the high energy photons to come out from a relativistic explosion. This requires initial bulk Lorentz factors of the radiating shell, $\gamma_0 \gtrsim 10^2$ (Piran 1999). Shemi & Piran (1990) pointed out that in the presence of even small amounts of baryons or *baryon contamination*, essentially the entire energy of the explosion gets locked up in the kinetic energy of the baryons, leaving little energy for the electromagnetic display. This problem was solved by Rees & Meszaros (1992) and independently by several authors (Narayan et al. 1992; Rees & Meszaros 1994; Paczynski & Xu 1994), by considering the reconversion of the kinetic energy of the fireball into radiation, due to interaction with an external medium or via internal shocks. However the allowed initial mass is still very small ($M \approx 10^{-6} M_\odot$), as too much baryonic mass will slow down the explosion and it will no longer be relativistic (Piran 1999). Hence, observation of a short bright pulse of γ -ray photons in GRBs require a very small amount of mass to be ejected with a very high bulk Lorentz factor.

The burst in the GRB itself results from the conversion of kinetic energy of ultra-relativistic particles or possibly the electromagnetic energy of a Poynting flux to radiation in an optically thin region. An inner engine is believed to accelerate the outflow to relativistic speeds, although the engine may remain hidden from direct observations. The “afterglow” on the other hand results from the slowing down of a relativistic shell on the external medium surrounding the progenitor star. There can also be an additional contribution to the afterglow from the inner engine that powers the GRB, since the engine may continue to emit energy for longer duration with a lower intensity and may produce the earlier part of the afterglow, say the first day or two in GRB 970228 and GRB 970508 (Piran 1999; Katz et al. 1998).

In supernovae associated with GRBs, after a brief high energy electromagnetic display, the relativistic ejecta continues to power a long lived radio afterglow (Kulkarni et al. 1998; Soderberg et al. 2004). Since the emergence of γ -ray photons, early in its evolution, constrains the initial relativistic ejecta mass to be very small and the initial bulk Lorentz factor to be very large, the relativistic ejecta sweeps up more circumstellar material than its own rest mass by the time the radio afterglow is detected. The evolution of the radiative blastwave has been described by Cohen et al. (1998). During the radio afterglow phase if radiative losses do not take away a significant fraction of the thermal energy, the blastwave may be treated as adiabatic. Under these conditions, the evolution of the blastwave is well described by the Blandford & McKee (1976) solution if the blastwave remains ultra-relativistic or by the Sedov-Taylor

solution if the blastwave has slowed down into the Newtonian regime. The interaction of GRBs with their circumstellar wind has been discussed by Chevalier & Li (2000). The spectra and light curves of GRB afterglows have been computed in the ultra-relativistic regime by Sari et al. (1998) and in the Newtonian regime by Frail et al. (2000).

Soderberg et al. (2010) have recently discovered bright radio emission, associated with the type Ibc SN 2009bb, requiring a substantial relativistic outflow powered by a central engine. The search for a γ -ray counterpart, spatially and temporally coincident with SN 2009bb, in data obtained from the all-sky Inter Planetary Network (IPN) of high energy satellites, did not detect a coincident GRB (Soderberg et al. 2010). The absence of detected γ -rays from this event relaxes the constraints of very high Lorentz factors and very low mass in the relativistic ejecta. In fact, the radio emitting outflow in SN 2009bb is mildly relativistic (Soderberg et al. 2010) and has a large baryonic mass coupled to it, as evidenced by the nearly free expansion for ~ 1 year (Figure 1). Since the swept up mass is still smaller than the rest mass of the relativistic ejecta, the evolution of the blastwave can neither be described by the the rapidly decelerating Blandford & McKee (1976) solution nor the Sedov-Taylor solution. Dermer & Chiang (1998); Chiang & Dermer (1999) have considered the emission from a collisionally decelerating blast wave as it transitions from nearly free expansion to the Blandford & McKee (1976) self similar solution. Huang et al. (1999) have discussed the subsequent transition to a Sedov-like phase.

Hence, the discovery of relativistic supernovae, such as SN 2009bb, without detected GRBs, relaxes the constraints from the *compactness problem* and *baryon contamination*. This motivates the study of highly baryon loaded mildly relativistic outflows which can remain in the nearly free expansion phase during the radio afterglow.

3. RELATIVISTIC BLASTWAVE SOLUTION

We use the simple collisional model described by Piran (1999); Chiang & Dermer (1999) where the relativistic ejecta forms a shell which decelerates through infinitesimal inelastic collisions with the circumstellar wind profile. The initial conditions are characterized by the rest frame mass M_0 of the shell launched by a CEDEX and its initial Lorentz factor γ_0 . In contrast to the self similar solutions, which describe the evolution away from the boundaries of the independent variables (Barenblatt & Zel'Dovich 1972) and the need for proper normalization to get the correct total energy, our set of initial conditions directly fixes the total energy as $E_0 = \gamma_0 M_0 c^2$.

3.1. Equations of Motion

The shell slows down by a sequence of infinitesimal inelastic collisions with the circumstellar matter. The swept up circumstellar matter is given by $m(R)$. Conservation of energy and momentum give us (see Chiang & Dermer 1999; Piran 1999),

$$\frac{d\gamma}{\gamma^2 - 1} = -\frac{dm}{M}, \quad (1)$$

and

$$dE = c^2(\gamma - 1)dm, \quad (2)$$

respectively, where dE is the kinetic energy converted into thermal energy, that is the energy in random motions as opposed to bulk flow, by the infinitesimal collision. In the adiabatic case this energy is retained in the shell and we have the analytic relation (from Piran 1999)

$$\frac{m(R)}{M_0} = -(\gamma_0 - 1)^{1/2}(\gamma_0 + 1)^{1/2} \times \int_{\gamma_0}^{\gamma} (\gamma' - 1)^{-3/2}(\gamma' + 1)^{-3/2} d\gamma'. \quad (3)$$

At the age of 17 days, the radio luminosity of SN 2009bb was $L_\nu \sim 5 \times 10^{28}$ ergs s $^{-1}$ Hz $^{-1}$ at 8.4 GHz (Soderberg et al. 2010). This implies a radio luminosity of $\nu L_\nu \sim 4.2 \times 10^{38}$ ergs s $^{-1}$. Compared with the energy in relativistic electrons of 1.3×10^{49} ergs (Soderberg et al. 2010), this gives a radiation timescale of $\sim 10^3$ years at age 17 days, which is very large compared to the age of the object. Hence, it is safe to compute the dynamics of the object in the adiabatic limit. We also note that since the available thermal energy initially grows with time as $E \propto R \propto t$ (shown later) and the luminosity falls off as $\nu L_\nu \propto t^{-1}$ (shown later) the adiabaticity condition only gets better with time. However, the radiation timescale would have been same as the age at $t \sim 70$ seconds, which is comparable to the duration of very Long Soft GRBs and XRFs.

For a circumstellar medium set up by a steady wind, where we expect a profile with $\rho \propto r^{-2}$, we have $m(R) = AR$ where A is the mass swept up by a sphere per unit radial distance. $A \equiv M/v_{wind}$ can be set up by a steady mass loss rate of \dot{M} with a velocity of v_{wind} from the pre-explosion CEDEX progenitor, possibly a Wolf Rayet star. Note that our definition of A is equivalent to $4\pi q$ in Equation (3 and 5) of Chevalier (1982). Integrating the right hand side then gives us

$$\frac{AR}{M_0} = \frac{\gamma\sqrt{\gamma_0^2 - 1}}{\sqrt{\gamma^2 - 1}} - \gamma_0. \quad (4)$$

For the physically relevant domain of $\gamma > 1$ this equation has only one analytical root at

$$\gamma = \frac{\gamma_0 M_0 + AR}{\sqrt{M_0^2 + 2A\gamma_0 R M_0 + A^2 R^2}}, \quad (5)$$

which gives the evolution of γ as a function of R . This is similar to Equation 8 of Chiang & Dermer (1999) for a adiabatic spherical blastwave in a wind like ($\rho \propto r^{-2}$) CSM profile. The amount of kinetic energy converted into thermal energy when the shell reaches a particular R can be obtained by integrating Equation (2) after substituting for γ from Equation (5) and $dm = AdR$, to get

$$E = c^2 \left(-M_0 - AR + \sqrt{M_0^2 + 2A\gamma_0 R M_0 + A^2 R^2} \right). \quad (6)$$

3.2. Evolution in Observer's Time

The evolution of R and γ can be compared with observations once we have the time in the observer's frame that corresponds to the computed R and γ . For emission along the line of sight from a blastwave with a constant γ the commonly used expression (Meszaros & Rees 1997) is

$$t_{obs} = \frac{R}{2\gamma^2 c}. \quad (7)$$

However, Sari (1997) has pointed out that for a decelerating ultra-relativistic blastwave the correct t_{obs} is given by the *differential* equation

$$dt_{obs} = \frac{dR}{2\gamma^2 c}. \quad (8)$$

We substitute γ from Equation (5) and integrate both sides to get the exact expression

$$t_{obs} = \frac{R(M_0 + A\gamma_0 R)}{2c\gamma_0(\gamma_0 M_0 + AR)}. \quad (9)$$

Note that, this reduces to the Meszaros & Rees (1997) expression only in the case of nearly free expansion and deviates as the shell decelerates. In the rest of the work we use t to indicate the time t_{obs} in the observer's frame. Inverting this equation and choosing the physically relevant *growing branch*, gives us the analytical time evolution of the line of sight blastwave radius, as

$$R = \frac{1}{2A\gamma_0} \times \left(-M_0 + 2Ac\gamma_0 t + \sqrt{8AcM_0 t \gamma_0^3 + (M_0 - 2Ac\gamma_0 t)^2} \right), \quad (10)$$

in the ultra-relativistic regime. This can now be substituted into Equations (5 and 6) to get the time evolution of the Lorentz factor γ and the thermal energy E (see Appendix). This gives us a complete solution for the blastwave time evolution, parametrized by the values for γ_0 , M_0 and A .

3.3. Series Expansions

Even though an analytical solution is at hand, it is instructive to look at the Taylor expansions in time for the relevant blastwave parameters of radius

$$R = 2c\gamma_0^2 t - \frac{4(Ac^2\gamma_0^3(\gamma_0^2 - 1))t^2}{M_0} + O(t^3), \quad (11)$$

Lorentz factor

$$\gamma = \gamma_0 - \frac{2(Ac\gamma_0^2(\gamma_0^2 - 1))t}{M_0} + O(t^2), \quad (12)$$

and thermal energy

$$E = 2Ac^3(\gamma_0 - 1)\gamma_0^2 t - \frac{2A^2c^4(3\gamma_0 - 2)\gamma_0^3(\gamma_0^2 - 1)t^2}{M_0} + O(t^3). \quad (13)$$

Equation (12) immediately tells us that the blastwave of a CEDEX starts out in a nearly free expansion phase, but slows down significantly by the time t_{dec} , when the first negative term in the Taylor expansion for γ becomes equal to γ_0 , where

$$t_{dec} = \frac{M_0}{2(Ac\gamma_0(\gamma_0^2 - 1))}. \quad (14)$$

This signals the end of the nearly free expansion phase and the solution enters a Blandford McKee like (see

Appendix B) or Sedov like phase, depending upon the Lorentz factor at that time.

4. BLASTWAVE ENERGETICS

We shall now use the blastwave solution developed in the previous section to predict the radio evolution of a CEDEX with a relativistic blastwave slowing down due to circumstellar interaction. For the prototypical SN 2009bb, the blastwave was only mildly relativistic at the time of the observed radio afterglow. In the absence of a significant relativistic beaming, the observer would receive emission from the entire shell of apparent lateral extent R_{lat} at a time t_{obs} given by

$$dt_{obs} = \frac{dR_{lat}}{\beta\gamma c}, \quad (15)$$

which is valid even in the mildly relativistic regime. Because of its mildly relativistic outflow, all expressions derived for SN 2009bb, use the above Equation rather than Equation 8 which is applicable in the ultra-relativistic case. In either case radio observations of SN 2009bb measure essentially the transverse R_{lat} not the line of sight R . Integrating term by term gives us the time evolution of the lateral radius as

$$R_{lat} = c\sqrt{\gamma_0^2 - 1}t - \frac{2(Ac^2\gamma_0^3\sqrt{\gamma_0^2 - 1})t^2}{M_0} + O(t^3). \quad (16)$$

The thermal energy available when the shell has moved out to a radius R is given exactly by Equation (6), however it is again convenient to look at its Taylor expansion,

$$E = Ac^2(\gamma_0 - 1)R - \frac{(A^2c^2(\gamma_0^2 - 1))R^2}{2M_0} + O(R^3). \quad (17)$$

4.1. Electron Acceleration

Sari et al. (1998) give the minimum Lorentz factor γ_m of the shock accelerated electrons as

$$\gamma_m = \epsilon_e \left(\frac{p-2}{p-1} \right) \frac{m_p}{m_e} \gamma. \quad (18)$$

At the mildly relativistic velocities seen in SN 2009bb, the peak synchrotron frequency of the lowest energy electrons are likely to be below the synchrotron self absorption frequency. This explains the $\nu^{5/2}$ low frequency behavior of the spectrum. Hence, considering an electron distribution with an energy spectrum $N_0 E^{-p} dE$, which we assume for simplicity to be extending from $\gamma_m m_e c^2$ to infinity, filling a fraction f of the spherical volume of radius R , we need an energy

$$E_e = \frac{4f(\gamma_m m_e c^2)^{1-p} N_0 \pi R^3}{3(p-1)}. \quad (19)$$

If a fraction $\epsilon_e \equiv E_e/E$ of the available thermal energy goes into accelerating these electrons, then for the leading order expansion of E in R the normalization of the electron distribution is given by

$$N_0 \simeq \frac{3Ac^2\epsilon_e(\gamma_0 - 1)(\gamma_m m_e c^2)^2}{2f\pi R^2}, \quad (20)$$

for $p = 3$, as inferred from the optically thin radio spectrum of SN 2009bb (Soderberg et al. 2010).

In the rest of this work we have made the simplifying assumption of a constant ϵ_e . The physics of shock acceleration is unlikely to change during time of interest as relevant parameters such as the shock velocity does not change much. Moreover, we show later in this work that the light curve of a CEDEX is controlled by the competition between a decreasing synchrotron flux at high frequencies and a decreasing optical thickness (hence increasing flux) at low frequencies. The major light curve features of a shifting peak frequency and a nearly constant peak flux, arise from this effect rather than micro-physical processes that may change ϵ_e .

4.2. Magnetic Field Amplification

If a magnetic field of characteristic strength B fills the same volume, it needs a magnetic energy of

$$E_B = \frac{1}{6} B^2 f R^3. \quad (21)$$

If a fraction $\epsilon_B \equiv E_B/E$ goes into the magnetic energy density, then the characteristic magnetic field is given by

$$B \simeq \frac{c}{R} \sqrt{\frac{6A\epsilon_B(\gamma_0 - 1)}{f}} \quad (22)$$

In the rest of this work, following the argument in the previous sub-section, we have made the simplifying assumption of a constant ϵ_B . This explains the observed $B \propto R^{-1}$ behavior (Figure 2) seen in SN 2009bb. These observations strengthens the case for a nearly constant ϵ_B . This feature of an explosion within a $\rho \propto r^{-2}$ wind profile is also seen in several non-relativistic radio supernovae. The normalization is given by the progenitor mass loss parameter, initial Lorentz factor, filling factor of the electrons and the efficiency with which the thermal energy is used in amplifying magnetic fields. Note that this phase would last only as long as the expansion is nearly free or $t < t_{dec}$. Therefore the observed $B - R$ relation in SN 2009bb argues for a $t_{dec} \gtrsim 1$ year and hence a CEDEX with a highly baryon loaded outflow.

Note that the highest energy to which a cosmic ray proton can be accelerated is determined by the $B R$ product (Hillas 1984; Waxman 2005). We have argued elsewhere (Chakraborti et al. 2010) that the mildly relativistic CEDEX are ideal for accelerating nuclei to the highest energies in sufficient volumetric energy injection rates and independent arrival directions to explain the post GZK cosmic rays. The above $B \propto R^{-1}$ dependence seen in Fig 2 implies that a CEDEX like SN 2009bb will continue to accelerate cosmic rays up to a nearly constant very high energy for long times, i.e. for the entire time that this (nearly free expansion) phase lasts.

5. ELECTRON SYNCHROTRON RADIO SPECTRUM

It is expected that the radio emission from a CEDEX will be produced by synchrotron emission of shock accelerated electrons in the shock amplified magnetic field quantified in the previous section. Once we have the evolution of N_0 and B , we can follow Chevalier (1998) to express the Synchrotron Self Absorbed (SSA) radio spectrum from a CEDEX in the optically thick regime using Rybicki & Lightman (1979) as

$$F_\nu = \frac{\pi R^2}{D^2} \frac{c_5}{c_6} B^{-1/2} \left(\frac{\nu}{2c_1} \right)^{5/2}, \quad (23)$$

where c_1 , c_5 and c_6 are constants given by Pacholczyk (1970) and D is the distance to the source. Similarly, the optically thin flux is given by

$$F_\nu = \frac{4\pi f R^3}{3D^2} c_5 N_0 B^{(p+1)/2} \left(\frac{\nu}{2c_1} \right)^{-(p-1)/2}, \quad (24)$$

In mildly relativistic cases such as SN 2009bb, we may receive radiation from the entire disk projected on the sky, hence R is to be understood as R_{lat} . Substituting for N_0 and B from Equations (20 and 22) and the leading order expansion for the projected lateral radius (Eq. 16), we have the optically thick flux as

$$F_\nu \simeq \left(c^2 c_5 (\gamma_0 - 1) (\gamma_0 + 1) \pi \left(\frac{\nu t}{c_1} \right)^{5/2} \right) \left(4c_6 D^2 \left(\frac{24A\epsilon_B}{\gamma_0 f + f} \right)^{1/4} \right). \quad (25)$$

Similarly, the optically thin flux can be expressed as

$$F_\nu \simeq \frac{24A^2 c^3 c_1 c_5 \epsilon_B \epsilon_e (\gamma_0 - 1)^2 (\gamma_m m_e c^2)^2}{(\nu t) D^2 f \sqrt{\gamma_0^2 - 1}}. \quad (26)$$

These equations together provide the flux density of a CEDEX as a function of time and frequency.

5.1. SSA Peak Frequency

The transition from the optically thick to optically thin regime happens at the peak frequency ν_p . At a fixed observation frequency this is reached in time t_p . The condition for the SSA peak may be obtained by equating the optically thin and thick flux, to get

$$\nu_p t_p \simeq 2^{23/14} 3^{5/14} \left(c c_6 \epsilon_e \sqrt[4]{\frac{A^9 \epsilon_B^5}{\gamma_0 f + f}} \sqrt{c_1^7 (\gamma_0^2 - 1)} \times (\gamma_m m_e c^2)^2 \frac{1}{\pi f (\gamma_0 + 1)^2} \right)^{2/7} \quad (27)$$

All quantities on the right hand side are constants or parameters of the problem which are uniquely fixed for a particular relativistic supernova. Hence, during the nearly free expansion phase $\nu_p \propto t_p^{-1}$ and the peak moves to lower and lower frequencies as the plasma expands and becomes optically thin with time. This behavior is also seen in the radio spectra of SN 2009bb.

The range in the values of $\nu_p t_p$ is then weakly dependent on the initial bulk Lorentz factor γ_0 and the mass loss rate, parametrized by A . The above expression can be used to select the frequency and cadence of radio follow-ups of type Ibc supernovae for detecting CEDEXs.

5.2. SSA Peak Flux

The peak flux density can now be obtained by substituting the expression for $\nu_p t_p$ into that for F_ν , to get,

$$F_{\nu_p} \simeq \left(2^{19/14} 3^{9/14} c^{19/7} c_5 \epsilon_B^{9/14} \epsilon_e^{5/7} (A f (\gamma_0 - 1))^{19/14} \times (\gamma_m m_e c^2)^{10/7} \pi^{2/7} \right) / \left(c_6^{2/7} D^2 f^2 \right). \quad (28)$$

This peak flux is obtained by keeping only the leading orders, for almost free expansion, is nearly a constant for for $t \ll t_{dec}$. As the blastwave slows down, the decay of the peak flux can be obtained exactly from the analytical expression for $R(t)$. However for simplicity a Taylor expansion can be written down as

$$\frac{F_{\nu p}(t)}{F_{\nu p}(0)} = 1 - \frac{5(Ac\gamma_0^3)t}{M_0} + O(t^{3/2}) \quad (29)$$

The peak flux may also come down if synchrotron losses for the electrons are significant. This would require a self consistent modeling of the time dependent acceleration and synchrotron losses of the relativistic electrons in the shock amplified magnetic field of a CEDEX blastwave.

The peak flux density $F_{\nu p}$ is then strongly dependent on the bulk Lorentz factor γ_0 and the parametrized mass loss rate, A . This suggests a large range in radio fluxes of CEDEXs and hence increased sensitivity of the Extended Very Large Array (EVLA) should help in detecting more of these enigmatic objects.

5.3. Synchrotron Cooling

Rybicki & Lightman (1979) give the characteristic synchrotron frequency of an electron with Lorentz factor $\gamma_e \gg 1$ in a magnetic field B as

$$\nu(\gamma_e) = \gamma_e^2 \frac{q_e B}{2\pi m_e c}. \quad (30)$$

Sari et al. (1998) provide the critical electron Lorentz factor γ_c , above which an electron will lose a significant portion of its energy within the age of the object, as

$$\gamma_c = \frac{6\pi m_e c}{\sigma_T \gamma B^2 t}. \quad (31)$$

Substituting this into Equation 30, we get the synchrotron cooling frequency as

$$\nu_c \equiv \nu(\gamma_c) = \frac{18\pi m_e c q_e}{\sigma_T \gamma B^3 t^2}. \quad (32)$$

Substituting the value of SN 2009bb magnetic field at 20 days from Table 1 of Chakraborti et al. (2010), we get the cooling frequency as ~ 2.6 THz. Since the magnetic field decays as $B \propto t^{-1}$, the cooling frequency will grow as $\nu_c \propto t$. Hence, synchrotron cooling is unimportant for electrons radiating near the SSA peak frequency $\nu_p \sim 7.6$ GHz, and they are indeed in the slow cooling regime during the timescale of interest.

The scaling relations for ν_c and ν_p show that they should have been comparable at around ~ 1 day and at a frequency of ~ 140 GHz. Very early time (~ 1 day) millimeter wave observations of CEDEXs are therefore encouraged. They may reveal the presence of a synchrotron cooling break in the radio spectrum. This may be used to determine the magnetic field independent of the equipartition argument (see Chandra et al. 2004a).

6. BLASTWAVE MODEL INVERSION

The input parameters of the model are specified by M_0 , γ_0 , A , ϵ_e and ϵ_B . Under the assumption of equipartition of the thermal energy between electrons, protons and magnetic fields we have $\epsilon_e = \epsilon_B = 1/3$. We then eliminate A between Equations (27 and 28) to get

$$\gamma_0^2 - 1 = 4 \left(\frac{3c_6^8 \epsilon_B (D^2 F_{\nu p})^9}{\pi^8 c_3^9 \epsilon_e f(\gamma_m m_e c^2)^2} \right)^{2/19} \left(\frac{c_1}{(\nu_p t_p) c} \right)^2, \quad (33)$$

which gives us the initial Lorentz factor γ_0 in terms of the early-time ($t \ll t_{dec}$) SSA peak frequency ν_p and the peak flux $F_{\nu p}$. In the non-relativistic limit this gives us

$$v \simeq 2 \left(\frac{3c_6^8 \epsilon_B (D^2 F_{\nu p})^9}{\pi^8 c_3^9 \epsilon_e f(\gamma_m m_e c^2)^2} \right)^{1/19} \left(\frac{c_1}{\nu_p t_p} \right), \quad (34)$$

which is insensitive to the equipartition parameter $\alpha \equiv \epsilon_e/\epsilon_B$ as $v \propto \alpha^{-1/19}$. The inferred γ_0 has a weak dependence on γ_m and is to be solved self consistently with Equation (18) giving us $\gamma_0 \simeq 1.16$ for SN 2009bb. Not doing so will incur an error in estimating the initial bulk Lorentz factor. Equations (33 or 34) may be used as a direct test of whether a radio supernova has relativistic ejecta.

The equipartition parameter α for a given CEDEX may be determined directly from radio observations if a synchrotron cooling break is seen in the broad band radio spectrum. Chandra et al. (2004a) have used this to determine the magnetic field in SN 1993J and its radial evolution (Chandra et al. 2004b), independent of the equipartition argument. Subsequently A (essentially the scaled mass loss rate) may be obtained by fitting Equation (22) to the B-R data (e.g. Figure 2). A direct method of estimating A would be to eliminate γ_0 between equations (27 and 28) to get $A \simeq 1.2 \times 10^{12}$ gram cm^{-1} . For a typical Wolf Rayet wind velocity of 10^3 km s^{-1} this density profile may be set up by a constant mass loss rate of $\dot{M} \simeq 1.9 \times 10^{-6} M_\odot \text{ yr}^{-1}$. This is consistent with the mass mass loss rate of the SN 2009bb progenitor already determined by Soderberg et al. (2010).

All CEDEXs at a given distance, in their nearly free expansion phase, are characterized by one of the constant γ_0 curves (Figure 4) and one of the constant \dot{M} curves (again Figure 4). This $F_{\nu p}$ vs $\nu_p t_p$ diagnostic plot for CEDEXs is essentially the relativistic analogue of Figure 4 of Chevalier (1998) where non-relativistic radio supernovae of different types are seen to lie on one of the constant velocity curves. For example, SN 2009bb, lies on a intermediate mass loss parameter A and a mildly relativistic γ_0 . For the same initial γ_0 as SN 2009bb, an object encountering lower circumstellar density, would be significantly fainter and faster evolving, such as those occurring near the points of intersection of the solid green curve and the dashed red curve. These objects, possibly at the faint end of the luminosity function of CEDEXs, may be discovered by a dedicated high sensitivity search for relativistic outflows from nearby type Ibc supernovae with the EVLA.

The ejecta mass can then be inferred from the deceleration timescale t_{dec} fitting the time evolution of the observed radii with the Taylor expansion (Equation 16) of R_{lat} obtained from our model. In Figure 1 we compare predictions from our model with the observed temporal evolution of the blastwave radius. The observed radii are consistent with a nearly free expansion for an apparent lateral velocity of $\gamma\beta = 0.527 \pm 0.022c$. As the ejecta has not yet slowed down significantly, it is not possible to determine M_0 but we can nevertheless put a lower limit on the ejecta mass. Models with M_0 below $10^{-2.5} M_\odot$ are ruled out at the 98.3% level by the observations of SN 2009bb. Hence, radio observations of a relativistic supernovae can constrain all the physically relevant parameters of our model.

7. COMPARISON WITH KNOWN SOLUTIONS

Blandford & McKee (1976) (hereafter BM) analyze the dynamics of both non-relativistic (NR) and ultra-relativistic (ER) blast waves in the adiabatic impulsive (AI) approximation as well as steady injection (SI) from a central power supply. A classification of the shock dynamics and the corresponding synchrotron and inverse Compton radiation from the strong relativistic spherical shock in an ionized magnetized medium is given by Blandford & McKee (1977). The dynamics of both NR and ER shocks are governed by the energy E of the adiabatic impulsive (AI) explosion; while in the case of steady injection of energy the dynamics is governed by Lt , where L is the luminosity of the central power supply. Other assumptions made by BM were that the shock is a strong one (see Footnote 2) and that the magnetic field is not dynamically important.

The external medium into which the shock wave expands can have radial variations of density. It can either be of uniform density or could be stratified into $\rho \propto r^{-k}$, with $k = 2$ for a constant velocity wind. The shock can be either adiabatic or radiative. In adiabatic shocks the radiative mechanisms are slow compared to hydrodynamics timescale, while in radiative shocks the radiative mechanisms are faster than the hydrodynamic timescale (measured in the observer-frame). A fully radiative blast wave may radiate away all the thermal energy generated by the shock, if for example, the external medium is composed mainly of electrons and positrons. Cohen et al. (1998) categorize shocks as “semi-radiative” in which the cooling is fast, but only a fraction of the energy is radiated away. This could take place in a collisionless shock acceleration, where the shock distributes the internal energy between the electrons and protons. After the material passes behind the shock, there is no coupling, effectively at the low densities behind the shock, between the electrons and protons. During the initial stage of the afterglow, the electrons may undergo synchrotron cooling or Compton scatter off low energy photons on timescales which are shorter than the dynamical timescale (Waxman 1997b; Meszaros et al. 1998; Sari et al. 1998), but the protons may not radiate and may remain hot. A narrow cooling layer may form behind the shock as in a fast cooling scenario even when the protons remain adiabatic and only the electrons cool. As the cooling parameter ϵ (the fraction of the energy flux lost in the radiative layer) increases, the matter concentrates in a small shell near the shock in the Newtonian solution; however in the ER case, even in the adiabatic case, the matter is concentrated in a narrow shell of width R/Γ^2 (where $\Gamma = \sqrt{2}\gamma$, is the ultra-relativistic shock wave Lorentz factor in the observer’s frame), but this concentration in a narrower denser shell increases with ϵ .

Classical fireball models of GRBs have a fully radiative stage during the (initial) γ -ray event with a radiative efficiency near unity and the implied energy is typically $E \sim 10^{51-52}$ erg and have a bulk Lorentz factor of $\Gamma \sim 10^2 - 10^3$. When the newly shocked electrons are radiating near the peak of the initial post-shock energy $\gamma_e \sim \xi_e(m_p/m_e)\Gamma(t)$ (here $\xi_e = O(1)$), they retain high radiative efficiency even after the GRB outburst for some time (Meszaros et al. 1998). If the protons establish

and remain in equipartition with the electrons throughout the entire remnant volume, the shock Lorentz factor evolves for a homogeneous external medium as: $\Gamma \propto r^{-3}$ (Blandford & McKee 1976). On the other hand, for the adiabatic regime where the radiative losses do not tap the dominant energy reservoir in protons and magnetic energy but only the electrons are responsible for the radiation, one has: $\Gamma \propto r^{-3/2}$ for a homogeneous medium (Meszaros et al. 1998).

For a NR blast wave of energy E into a medium of density ρ_0 in the Sedov-Taylor phase, it is possible to construct a characteristic velocity at a time t from the combination $(E/\rho_0 t^3)^{1/5}$. For the relativistic problem, as BM point out, an additional velocity the speed of light is introduced into the problem. The mean energy per particle in the shocked fluid varies as Γ^2 , where one factor of Γ arise from the increase in energy measured in the co-moving frame and the second arise from a Lorentz transformation into the fixed (i.e. the observer) frame. When most of the energy is resides in recently shocked particles, the total energy is proportional to $\Gamma^2 R^3$. Here R is the current shock radius. If the total energy contained in the shocked fluid is to remain constant, then $\Gamma^2 \propto t^{-3}$. One can consider a more general case in which the energy is supplied continuously at a rate proportional to a power of the time and set:

$$\Gamma^2 \propto t^{-m} \text{ for } m > -1. \quad (35)$$

For the $m=3$ case, corresponding to an impulsive injection of energy into the blast wave on a time scale short compared with R , the total energy can be shown to be given by:

$$E = 8\pi w_1 t^3 \Gamma^2 / 17, \quad (36)$$

where w_1 is the enthalpy ahead of the shock, so that with $\Gamma^2 \propto t^{-3}$, the total energy is indeed a constant in time in the fixed frame.

BM also provide a solution for an ER adiabatic blast wave in an external density gradient $\rho_1 \propto n_1 \propto r^{-k}$ but with a cold, pressure-less external medium. This is the case for a blast wave propagating through a spherically symmetric wind. For this example they find that for $k=2$, $m=1$ corresponds to an impulsive energy injection due to a blast wave in a constant velocity wind. In this case, the analytic solution to the adiabatic impulsive blast waves can be obtained for $m = 3 - k > -1$, and the total energy in this case is:

$$E = 8\pi \rho_1 \Gamma^2 t^3 / (17 - 4k). \quad (37)$$

Again this energy is constant to the lowest order in Γ^{-2} .

We compare our solution to other well known analytic and numerical schemes in the two final Figures. The graphs are not really for SN 2009bb-like systems. As they are for a baryon loaded explosion with a γ_0 of 300 going into a wind-like CSM. There may not be any such spherical explosions with these kind of energies. The comparison in these figures are not for any physically relevant objects (or scenarios) but rather for the purpose of showing the consistency of our analytical solutions with previously reported numerical techniques and known real asymptotic or intermediate asymptotic solutions.

In Figure 5 we compare our solution, in the ultra-relativistic regime with nearly free expansion or the coasting solution at early times and a BM like solution

at intermediate times. The blast wave solution for the special case of adiabatic impulsive solution for a constant velocity wind obtained in Section 3 is valid for arbitrary values of M_0 and γ_0 and the mass loss parameter A . The corresponding solutions in the Blandford McKee analysis can be obtained from our exact solution in the limit of small initial mass of the high velocity ejecta $M_0 \ll m(R)\gamma_0$ where $m(R)$ is the swept-up mass in the wind. Thus Equation (B1) shows that our intermediate asymptotic expressions for R and γ have the same time dependence as those of the BM solution. Similarly, the opposite limit $M_0 \gg m(R)\gamma_0$ gives a nearly free expansion of the blast wave. Thus the relativistic CEDEX which had relatively low mass (although the prototype SN 2009bb was still significantly baryon loaded compared to classical GRBs), underwent nearly free expansion initially. This is the relativistic analogue of the Chevalier (1982); Nadezhin (1985) phase of the non-relativistic supernovae. Eventually, an ultra-relativistic CEDEX would enter the Blandford-McKee phase (the relativistic analogue of the Sedov-Taylor phase) when it has swept up enough mass from the external medium surrounding the CEDEX.

In Figure 6 we compare our solution, in the mildly-relativistic regime with a BM like solution at intermediate times and a Snowplough phase at late times. The BM-like phase becomes unphysical when γ approaches 1 (hence β becomes 0) and the Snowplough phase is feasible only much later when β is less than 1. Both Figures also compare our solution to a direct numerical solution of the equations of motion computed for this work, under under the relevant conditions as prescribed by Chiang & Dermer (1999). These Figures demonstrate that patched solutions are much worse than the solution proposed here or even numerical solutions. While there can be a patch (though worse than our solution) between coasting and BM, there exists no patch between BM and Snowplough. While our analysis is for a wind like ($\rho \propto r^{-2}$) medium, see Kobayashi et al. (1999) for similar transitions seen in numerical simulations of the evolution of an adiabatic relativistic blastwave in a uniform medium.

Our framework may be used in the future to study the transition of a relativistic blastwave into a non relativistic Sedov phase. Frail et al. (2000) have used the Sedov phase for very late time calorimetry of GRB 970508. The relation between the blast wave radius and the observer's frame time also leads to the appropriate numerical factor connecting the two for a $\rho \propto r^{-2}$ exterior (See Appendix B). Note the different results in the literature due to Sari (1997); Waxman (1997a) for an uniform media.

8. DISCUSSIONS

Explosion dynamics where adiabatic, ultra-relativistic or trans-relativistic outflow takes place in a wind-like CSM can be classified in a parameter space spanned by M_0 , γ_0 and A , i.e. the initial ejected mass, bulk Lorentz factor of the ejecta and the mass loss parameter of the external wind established before the explosion, apart from the electron acceleration and magnetic field amplification efficiencies parametrized by ϵ_e and ϵ_B . At low γ_0 , we have the non relativistic supernovae, which usually have considerable ejecta mass (e.g. at least $0.1 M_\odot$, often much larger). If the progenitor of the SN has

had very heavy mass loss soon before the explosion took place, then an initially free expansion of the shock quickly sweeps up a mass equal to or greater than M_0 and the explosion enters the Sedov-Taylor like phase. Alternately a low ejecta mass initially would also lead to the early onset of the S-T phase.

The long duration GRB afterglows are powered by explosions that have very small initial ejecta mass, typically $10^{-6} M_\odot$. Comparatively, the initial mass of the ejecta in SN 2009bb estimated in Section 6 is considerably larger at $M_0 > 10^{-2.5} M_\odot$, but not as large as non-relativistic supernovae. These explosions are therefore baryon loaded. As baryon loading is a factor that affects the conversion of the impulsive release of energy into kinetic energy of the matter around the central source, this can quench the emergence of the gamma-rays in a burst. The substantial baryon loading in SN 2009bb compared to classical GRBs may in fact have played a significant role in the circumstance that no gamma-rays were in fact seen from this CEDEX, despite a thorough search by a suite of satellites in the relevant time window. At the same time, the CEDEX, such as SN 2009bb, are also unique in that they span a region of γ_0 which is trans-relativistic. So far the LGRBs and the corresponding outflows were being described in the extreme relativistic limit as in BM. Here we provide a solution of the relativistic hydrodynamics equations which is uniquely tuned to the CEDEX class of objects like SN 2009bb. Because of the non-negligible initial ejecta mass of such a CEDEX, objects like this would persist in the free expansion phase for quite a long time into their afterglow. Sweeping up a mass equal to that of the original ejecta would take considerable time, unless the mass loss scale in its progenitor was very intense, i.e. it had a large A .

In this paper we also provide an analysis of the peak radio flux versus the product of the peak radio frequency and the time to rise to the radio peak. There are loci in this plane that are spanned by low, intermediate and high velocity explosions. Radio SNe, LGRBs and CEDEXs are seen to occupy different niches in this plane. Similarly, we provide expressions for the peak fluxes and peak radio frequencies in terms of mass-loss factors of the explosions. We also invert their dependence on γ_0 and \dot{M} in terms of the peak frequency, peak time and peak fluxes to interpret the parameters of the explosion. We have also demonstrated that a seed magnetic field amplified by the shock as described above plays a crucial role in the generation of synchrotron radiation and have argued (Chakraborti et. al, in prep) that the acceleration of cosmic rays to ultra-high energies is possible in SN 2009bb-like objects.

We thank Alicia Soderberg, Abraham Loeb and Poonam Chandra for discussions on mildly relativistic supernovae. We thank Naveen Yadav for checking the manuscript and Swastik Bhattacharya for help with mathematics. This work has made use of the Wolfram Mathematica computer algebra system. This research was supported by the TIFR 11th Five Year Plan Project no. 11P-409. We thank the Institute for Theory and Computation, Harvard University for its hospitality. We thank an anonymous referee for detailed comments which significantly extended this work, in particular for point-

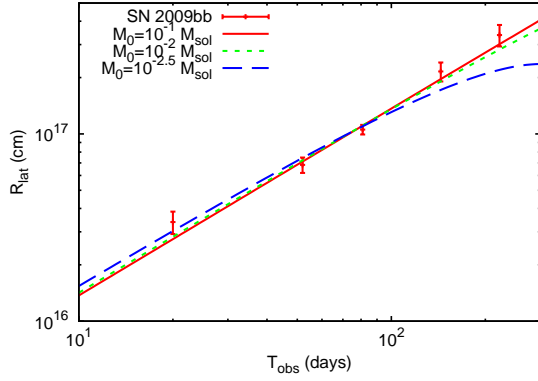


FIG. 1.— Evolution of the blast wave radius R_{lat} , determined from SSA fit to observed radio spectrum, as a function of the time t_{obs} in the observer's frame. The evolution is consistent with nearly free expansion. Note that the observations require $M_0 \gtrsim 10^{-2.5} M_{\odot}$.

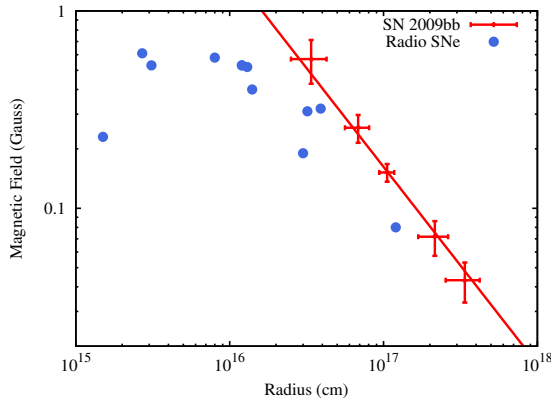


FIG. 2.— Magnetic field as a function of blast wave radius, as determined from SSA fits. Blue dots represent size and magnetic field of radio supernovae from Chevalier (1998) at peak radio luminosity. Red crosses (with 3σ error-bars) give the size and magnetic field of SN 2009bb at different epochs, from spectral SSA fits. Red line gives the best $B \propto R^{-1}$ (Equation 22) fit.

ing out to us the Chiang and Dermer papers, which we were unaware of. We thank Charles Dermer for sharing their numerical results in these papers. We thank Tsvi Piran and Charles Dermer for discussions at the Annapolis GRB2010 meeting.

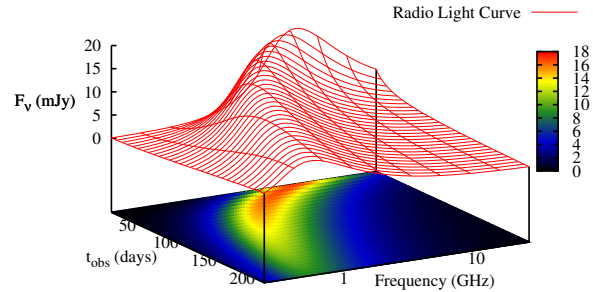


FIG. 3.— The flux density F_{ν} as a function of the frequency ν and the time in the observer's frame t_{obs} , as predicted from the model proposed in this work. The values used for the parameters, are those of SN 2009bb.

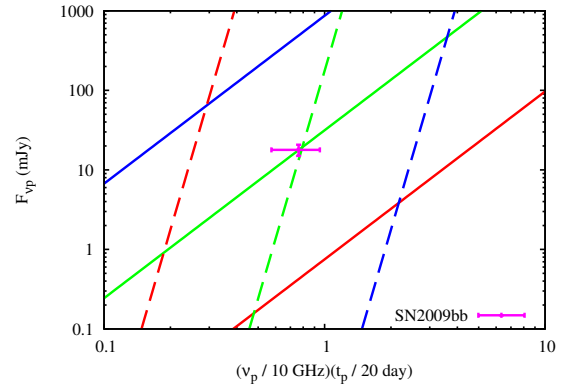


FIG. 4.— Diagnostic $F_{\nu p}$ vs $\nu_p t_p$ plot of our fiducial CEDEX in the nearly free expansion phase, at a distance of 40 Mpc. Solid lines from right to left represent loci of constant $\gamma_0 = 1.005$ (Red), 1.16 (Green) and 3.0 (Blue), traced by keeping the LHS of Equation D1 fixed at the respective values. Dashed lines from right to left represent loci of constant $\dot{M} = 0.2$ (Red), 1.9 (Green) and 20 (Blue) in units of $10^{-6} M_{\odot} \text{yr}^{-1}$, again traced by keeping the LHS of Equation D2 fixed at the respective values. The cross marks the set of values derived for the prototypical SN 2009bb spectrum from Soderberg et al. (2010) at 20 days, with 3σ error-bars. Radio observations can be used to deduce the initial bulk Lorentz factor γ_0 of a CEDEX and the pre-explosion mass loss rate \dot{M} from this diagram.

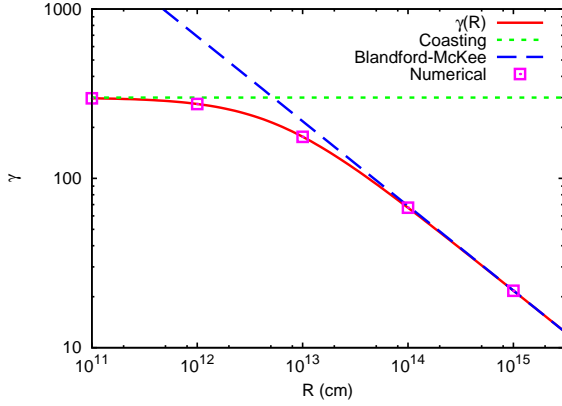


FIG. 5.— Early time radial evolution of the bulk Lorentz factor $\gamma(R)$ in a CEDEX, derived in Equation 5 of this work (red solid line), as compared to an initial nearly free expansion or coasting phase (green dotted line) and the intermediate Blandford-McKee like phase (blue dashed line). Magenta squares represent a direct numerical solution of the equations of motion following the method prescribed by Chiang & Dermer (1999). Note the transition from a coasting phase to the Blandford-McKee like phase.

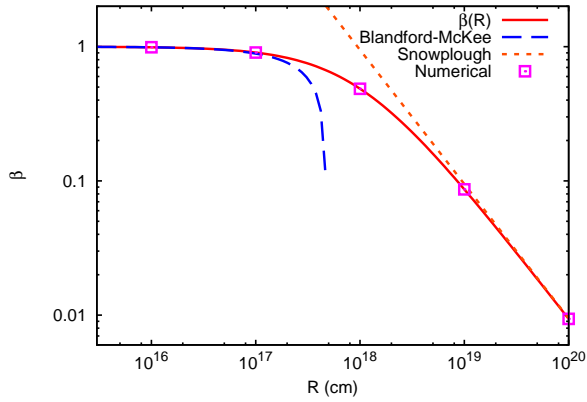


FIG. 6.— Late time radial evolution of $\beta(R) = v(R)/c$ in a CEDEX, derived using Equation 5 of this work (red solid line), as compared to an intermediate Blandford-McKee like phase (blue dashed line) and a final Snowplough phase (orange dotted line). Magenta squares represent a direct numerical solution of the equations of motion following the method prescribed by Chiang & Dermer (1999). Note the transition from the Blandford-McKee like phase to a Newtonian Snowplough phase.

APPENDIX

A. TEMPORAL EVOLUTION OF BLASTWAVE PARAMETERS

The evolution of the blastwave radius has already been shown to be given by

$$R = \frac{-M_0 + 2Ac\gamma_0 t + \sqrt{8AcM_0 t \gamma_0^3 + (M_0 - 2Ac\gamma_0 t)^2}}{2A\gamma_0}. \quad (\text{A1})$$

This can be substituted into into Equations (5) to get

$$\gamma = \left(\gamma_0 M_0 + \frac{-M_0 + 2Ac\gamma_0 t + \sqrt{8AcM_0 t \gamma_0^3 + (M_0 - 2Ac\gamma_0 t)^2}}{2\gamma_0} \right) / \sqrt{\left(2Ac\gamma_0 t + \sqrt{8AcM_0 t \gamma_0^3 + (M_0 - 2Ac\gamma_0 t)^2} \right) M_0 + \frac{\left(-M_0 + 2Ac\gamma_0 t + \sqrt{8AcM_0 t \gamma_0^3 + (M_0 - 2Ac\gamma_0 t)^2} \right)^2}{4\gamma_0^2}}, \quad (\text{A2})$$

which gives the time evolution of the Lorentz factor γ . The amount of kinetic energy converted into thermal energy E is similarly obtained by substituting $R(t)$ into Equations (6) to get

$$E = c^2 \left(-M_0 + \frac{M_0 - 2Ac\gamma_0 t - \sqrt{8AcM_0 t \gamma_0^3 + (M_0 - 2Ac\gamma_0 t)^2}}{2\gamma_0} + \sqrt{\left(2Ac\gamma_0 t + \sqrt{8AcM_0 t \gamma_0^3 + (M_0 - 2Ac\gamma_0 t)^2} \right) M_0 + \frac{\left(-M_0 + 2Ac\gamma_0 t + \sqrt{8AcM_0 t \gamma_0^3 + (M_0 - 2Ac\gamma_0 t)^2} \right)^2}{4\gamma_0^2}} \right) \quad (\text{A3})$$

Together, these three equations describe the temporal evolution of the blastwave parameters. However, for times less than t_{dec} , it is sufficient to use the first few Taylor coefficients, to derive the leading order behavior of the observable quantities.

B. ULTRA-RELATIVISTIC LIMIT FOR NEGLIGIBLE EJECTA MASS

Blandford & McKee (1976) describe the self similar evolution of an ultra-relativistic blastwave in the $\gamma \gg 1$ limit. This is the relativistic analog of the non-relativistic Sedov-Taylor solution as the ejecta mass is considered negligible compared to the swept up mass. Blandford & McKee (1976) provide a generalization of their solution to a blastwave plowing through a $\rho \propto r^{-k}$ circumstellar profile. This is of particular interest for the $k = 2$ constant wind profile, relevant for the early evolution of some GRB afterglows. For this situation, their solution provides a self similar evolution with $R \propto t^{1/2}$ and $\gamma \propto t^{-1/4}$ (see Piran 2004, Equation 77 with $k = 2$).

Barenblatt & Zel'Dovich (1972) have pointed out that self similar solutions do not merely represent specific solutions, but describe the intermediate asymptotic behavior of a wider class of solutions away from the boundaries of the independent variables. Hence, we investigate the low ejecta-mass limit ($\lim M_0 \rightarrow 0$) in our model, keeping the initial energy $E_0 = \gamma_0 M_0 c^2$ constant and obtain from Equations (A1 and A2)

$$R \simeq \left(\frac{2E_0}{Ac} \right)^{1/2} t^{1/2}, \quad \gamma \simeq \left(\frac{E_0}{2^3 Ac^3} \right)^{1/4} t^{-1/4}. \quad (\text{B1})$$

Hence the ultra-relativistic Blandford-McKee solution for a $\rho \propto r^{-2}$ circumstellar media is a special limiting case of the general solution obtained in this work. Our Equations (A1 and A2) track the evolution of the blastwave from nearly free expansion ($M_0 \gg m(R)\gamma_0$) into the Blandford-McKee phase ($M_0 \ll m(R)\gamma_0$). Note that unlike the self similar solutions (eg. Equation B1) there is no divergence in quantities like the bulk Lorentz Factor at the $t = 0$ boundary of our solution (eg. Equation A2). As the result γ_0 is bounded above, by total energy considerations.

Note that Equations (B1) together imply a unique relation between the blastwave radius and the time in the observer's frame, $t_{obs} = R/(4\gamma^2 c)$, which is different from the commonly used expression (Equation 7) given by Meszaros & Rees (1997) by a factor of 2. The corresponding relation in case of a uniform external medium has been argued over by Sari (1997); Waxman (1997a).

C. STIR-FRY EXPRESSIONS: RADIO SPECTRUM IN NEARLY FREE EXPANSION PHASE

The relativistic outflow in the prototypical SN 2009bb was discovered from its strong radio emission (Soderberg et al. 2010). Hence, more such objects may be uncovered in radio follow up of type Ibc supernovae. Equations (27 and 28)

completely describe the early ($t \lesssim t_{dec}$) temporal evolution of the radio afterglow of a CEDEX. However, instead of expressing $F_{\nu p}$ and ν_p in CGS units in terms of many constants, it would be of use to express them in units commonly used by radio observers. Hence, substituting for the fundamental constants and replacing for the appropriate choice of c_1 , c_5 and c_6 from Pacholczyk (1970), we express the peak flux density as

$$F_{\nu p} \simeq 87 \times \left(\frac{\epsilon_B}{0.33}\right)^{9/14} \left(\frac{\epsilon_e}{0.33}\right)^{5/7} \left(\frac{f}{0.5}\right)^{-9/14} (\gamma_0 - 1)^{19/14} \\ \times \left(\frac{D}{40 \text{ Mpc}}\right)^{-2} \left(\left(\frac{\dot{M}}{10^{-6} M_\odot}\right) \left(\frac{v_{wind}}{10^3 \text{ kms}^{-1}}\right)^{-1}\right)^{19/14} \text{ mJy.} \quad (\text{C1})$$

Here, the fiducial values of the parameters are chosen from those appropriate for the prototypical SN 2009bb. Similarly, the temporal evolution of the SSA peak frequency is given by,

$$\nu_p \simeq 9.5 \times \left(\frac{t_{obs}}{20 \text{ days}}\right)^{-1} \left(\frac{\epsilon_B}{0.33}\right)^{5/14} \left(\frac{\epsilon_e}{0.33}\right)^{2/7} \left(\frac{f}{0.5}\right)^{-5/14} (\gamma_0^2 - 1)^{1/7} \\ \times (\gamma_0 + 1)^{-9/14} \left(\left(\frac{\dot{M}}{10^{-6} M_\odot}\right) \left(\frac{v_{wind}}{10^3 \text{ kms}^{-1}}\right)^{-1}\right)^{9/14} \text{ GHz.} \quad (\text{C2})$$

Given the model parameters, these equations together describe the peak radio flux density of a CEDEX and the time evolution of its SSA peak in the nearly free expansion phase. The flux density at any frequency ν and time t , can then be expressed as

$$F_\nu(t) \simeq \begin{cases} F_{\nu p} \left(\frac{\nu}{\nu_p(t)}\right)^{5/2} & \text{if } \nu < \nu_p, \text{ or} \\ F_{\nu p} \left(\frac{\nu}{\nu_p(t)}\right)^{-(p-1)/2} & \text{if } \nu \geq \nu_p, \end{cases} \quad (\text{C3})$$

in terms of the already computed $F_{\nu p}$ and ν_p , where an electron index of $p \approx 3$, is appropriate for a SN 2009bb-like spectrum with a optically thin spectral index of $\alpha \approx -1$. These expressions also should be useful in designing radio surveys aimed at detecting CEDEXs.

D. EXTRACTING BLAST WAVE PARAMETERS FROM RADIO OBSERVATIONS

The inverse problem is that of determining the initial bulk Lorentz factor specified by γ_0 , progenitor mass loss rate given by \dot{A} or \dot{M} and the initial ejecta mass M_0 , from the radio observations. The bulk Lorentz factor may be determined from the radio observations using Equation (33) to get the simplified expression for γ_0 as,

$$\gamma_0^2 \simeq 1 + 0.225 \times \left(\frac{\epsilon_B}{\epsilon_e}\right)^{2/19} \left(\frac{f}{0.5}\right)^{-2/19} \left(\frac{t_{obs}}{20 \text{ days}}\right)^{-2} \left(\frac{\nu_p}{10 \text{ GHz}}\right)^{-2} \left(\frac{F_{\nu p}}{20 \text{ mJy}}\right)^{18/19} \left(\frac{D}{40 \text{ Mpc}}\right)^{36/19}. \quad (\text{D1})$$

The result is insensitive to the equipartition parameter $\alpha \equiv \epsilon_e/\epsilon_B$ and filling fraction f . This may be used to reliably determine the initial bulk Lorentz factor of a radio detected CEDEX in the mildly relativistic, nearly free expansion phase (like SN 2009bb).

An expression for $A \equiv \dot{M}/v_{wind}$, the circumstellar density profile, set up by the mass loss from the progenitor may be obtained by eliminating γ_0 between equations (27 and 28). This gives us a complicated algebraic dependence on $F_{\nu p}$ and $\nu_p t_p$. Since $\nu_p t_p$ is a pure number $\gg 1$, we can expand this expression in an asymptotic series (Erdelyi 1956) around $\lim \nu_p t_p \rightarrow \infty$. This gives us the approximate expression for the mass loss rate as

$$\dot{M} \simeq 3.0 \times 10^{-6} \left(\frac{\epsilon_B}{0.33}\right)^{-11/19} \left(\frac{\epsilon_e}{0.33}\right)^{-8/19} \left(\frac{f}{0.5}\right)^{11/19} \left(\frac{v_{wind}}{10^3 \text{ kms}^{-1}}\right)^1 \\ \times \left(\frac{t_{obs}}{20 \text{ days}}\right)^2 \left(\frac{\nu_p}{10 \text{ GHz}}\right)^2 \left(\frac{F_{\nu p}}{20 \text{ mJy}}\right)^{-4/19} \left(\frac{D}{40 \text{ Mpc}}\right)^{-8/19} M_\odot \text{ yr}^{-1}. \quad (\text{D2})$$

This approximate expression indicates the dependence of the inferred mass loss rate on the observational parameters, and makes an error of only $\lesssim 10\%$ in case of SN 2009bb, when compared to the exact expression. Given the uncertainties in the observations, we recommend the use of this expression to get an estimate of the mass loss rate from a CEDEX progenitor. Note that, this expression has similar scaling relations as Equation (23) of Chevalier & Fransson (2006). Hence, the mass loss rate of SN 2009bb as determined using that equation by Soderberg et al. (2010) remains approximately correct.

The initial ejecta rest mass M_0 cannot be estimated from radio observations in the nearly free expansion phase. It can only be determined when the CEDEX ejecta slows down sufficiently due to interaction with the circumstellar matter (Figure 1). Thereafter, the initial ejecta mass can be obtained from the Equation (14) using the timescale of slowdown t_{dec} and the already determined A and γ_0 . Nearly free expansion for a particular period of time, can only put lower limits on the ejecta mass, as shown in this work.

E. ANGULAR SIZE EVOLUTION AND VLBI

Very Long Base Interferometric (VLBI) measurements of the apparent angular diameters may be compared to the predicted value of R_{lat} , as a direct test of the CEDEX model. In the nearby universe, where the luminosity distance and the angular distance are not significantly different, we can substitute Equation (D1) into Equation (16) to obtain the predicted angular diameter $\theta \simeq 2R_{lat}/D$ of a CEDEX as,

$$\theta \simeq 82 \times \left(\frac{\epsilon_B}{\epsilon_e}\right)^{1/19} \left(\frac{f}{0.5}\right)^{-1/19} \left(\frac{\nu_p}{10 \text{ GHz}}\right)^{-1} \left(\frac{F_{\nu p}}{20 \text{ mJy}}\right)^{9/19} \left(\frac{D}{40 \text{ Mpc}}\right)^{-1/19} \mu\text{as}. \quad (\text{E1})$$

This expression which is insensitive to the equipartition parameter, the filling factor and even the assumed distance to the source, may be used in planning VLBI observations of a radio detected CEDEX and for comparing the observed angular sizes with those predicted from our model.

At $t_{obs} \simeq 81$ days post explosion, the radio spectrum of SN 2009bb, constructed from broadband Giant Metrewave Radio Telescope (GMRT) and Very Large Array (VLA) observations, as given by Soderberg et al. (2010) is well fit by an SSA spectrum with $F_{\nu p} = 10.82 \pm 0.34$ mJy and $\nu_p = 1.93 \pm 0.07$ GHz. Substituting these values into Equation (E1) we have the angular diameter as $\theta = 318 \pm 12 \mu\text{as}$, for the fiducial values of f , ϵ_B and ϵ_e adopted in this work. Hence, the angular radius of 0.16 mas predicted by our model is consistent with the 3σ upper limit (Bietenholz et al. 2010) of 0.64 mas reported from VLBI observations at around $t_{obs} \simeq 85$ days. Bietenholz et al. (2010) adopt a Sedov-Taylor expansion for the blastwave, according to which the source will not be resolved anytime soon. However, our model indicates a nearly free, mildly relativistic expansion for SN 2009bb, which may soon be resolvable at the VLBI scale. We note, by $t_{obs} \simeq 222$ days, the radio spectrum had evolved to $F_{\nu p} = 8.35 \pm 0.59$ mJy and $\nu_p = 0.53 \pm 0.04$ GHz, predicting an angular radius of around 0.51 mas according to Equation (E1). We therefore predict that a careful VLBI observation will now successfully resolve the radio emission from SN 2009bb and confirm the nearly free expansion indicated by our analytic solution. Given the lower fluxes at the usually high VLBI frequencies, this may be a challenging observation due to inadequate sensitivity and unsuitability of self-calibration techniques at low fluxes.

REFERENCES

- Barenblatt, G. I., & Zel'Dovich, Y. B. 1972, Annual Review of Fluid Mechanics, 4, 285
- Bietenholz, M. F., et al. 2010, ArXiv e-prints
- Blandford, R. D., & McKee, C. F. 1976, Physics of Fluids, 19, 1130
- . 1977, MNRAS, 180, 343
- Chakraborti, S., Ray, A., Soderberg, A., Loeb, A., & Chandra, P. 2010, arXiv:astro-ph/1012.0850
- Chandra, P., Ray, A., & Bhatnagar, S. 2004a, ApJ, 604, L97
- . 2004b, ApJ, 612, 974
- Chevalier, R. A. 1982, ApJ, 259, 302
- . 1998, ApJ, 499, 810
- Chevalier, R. A., & Fransson, C. 2006, ApJ, 651, 381
- Chevalier, R. A., & Li, Z. 2000, ApJ, 536, 195
- Chiang, J., & Dermer, C. D. 1999, ApJ, 512, 699
- Cohen, E., Piran, T., & Sari, R. 1998, ApJ, 509, 717
- Dermer, C. D., & Chiang, J. 1998, New Astronomy, 3, 157
- Erdelyi, A. 1956, Asymptotic Expansions (Dover Publications)
- Frail, D. A., Waxman, E., & Kulkarni, S. R. 2000, ApJ, 537, 191
- Goodman, J. 1986, ApJ, 308, L47
- Hillas, A. M. 1984, ARA&A, 22, 425
- Huang, Y. F., Dai, Z. G., & Lu, T. 1999, MNRAS, 309, 513
- Katz, J. I., Piran, T., & Sari, R. 1998, Physical Review Letters, 80, 1580
- Kobayashi, S., Piran, T., & Sari, R. 1999, ApJ, 513, 669
- Kulkarni, S. R., et al. 1998, Nature, 395, 663
- Meszáros, P., & Rees, M. J. 1997, ApJ, 476, 232
- Meszáros, P., Rees, M. J., & Wijers, R. A. M. J. 1998, ApJ, 499, 301
- Nadezhin, D. K. 1985, Ap&SS, 112, 225
- Narayan, R., Paczynski, B., & Piran, T. 1992, ApJ, 395, L83
- Paczolczyk, A. G. 1970, Radio astrophysics. Nonthermal processes in galactic and extragalactic sources, ed. Paczolczyk, A. G.
- Paczynski, B. 1986, ApJ, 308, L43
- Paczynski, B., & Xu, G. 1994, ApJ, 427, 708
- Piran, T. 1999, Phys. Rep., 314, 575
- . 2004, Reviews of Modern Physics, 76, 1143
- Rees, M. J., & Meszáros, P. 1992, MNRAS, 258, 41P
- . 1994, ApJ, 430, L93
- Rhoads, J. E. 1999, ApJ, 525, 737
- Ruderman, M. 1975, Annals of the New York Academy of Sciences, 262, 164
- Rybicki, G. B., & Lightman, A. P. 1979, Radiative processes in astrophysics, ed. Rybicki, G. B. & Lightman, A. P.
- Sari, R. 1997, ApJ, 489, L37
- Sari, R., Piran, T., & Narayan, R. 1998, ApJ, 497, L17
- Schmidt, W. K. H. 1978, Nature, 271, 525
- Sedov, L. I. 1946, Journal of Applied Mathematics and Mechanics, 10, 241
- Shemi, A., & Piran, T. 1990, ApJ, 365, L55
- Soderberg, A. M., et al. 2004, Nature, 430, 648
- . 2010, Nature, 463, 513
- Taylor, G. 1950, Royal Society of London Proceedings Series A, 201, 159
- von Neumann, J. 1963, The point source solution, ed. Taub, A. J. (Permagon Press), 219–237
- Waxman, E. 1997a, ApJ, 491, L19
- . 1997b, ApJ, 485, L5
- . 2005, Physica Scripta Volume T, 121, 147